Hindawi
Geofluids
Volume 2022, Article ID 3851806, 19 pages
https://doi.org/10.1155/2022/3851806

Research Article

The Evolutionary Characteristics of Lower Permian Keziliqiman Reefs in the Southwest Margin of Tarim Basin, Northwest China

Yijun Wang, Hongming Tang, Guang Yang, Zhenyu Wang, Yunfeng Zhang, and Lei Chen

School of Geoscience and Technology, Southwest Petroleum University, Chengdu, Sichuan 610500, China

Correspondence should be addressed to Hongming Tang; 201711000029@stu.swpu.edu.cn

Received 9 June 2022; Accepted 19 July 2022; Published 4 August 2022

Academic Editor: Yuxiang Zhang

The Permian strata in the southwest Tarim Basin contain organic reefs with good exploration prospects. Based on observations of outcrops and thin section examination of the Permian Keziliqiman Formation reef in the Sangzhu section of Pishan County, Xinjiang, northwest China, the basic characteristics of the reef are studied. This organic reef, as a point reef which grew along the platform margin, has a complete subfacies system of base, core, front, back, and cap. The lithology of the lower zone of the core is mainly sponge bafflestone, while that of the upper zone is coral framestone. The development of reefs was controlled by the rise and fall of sea level. It was when the sea level rose in southwest Tarim Basin that the Keziliqiman reef gradually came into existence. Later, with rapid decline of sea level in that area, the Sangzhu section turned into a hot and dry supratidal zone, where algae began to flourish, dolomitization intensified, reef building organisms died en masse, and eventually the reef died. Paleontological and geochemical characteristics of the Sangzhu reef indicate that the sea-level decline in southwest Tarim Basin may be related to the Early Permian glaciers. Since then, the reef began to be transformed by diagenesis. But on the whole, its effect was not significant. Furthermore, its diagenetic process had more to do with marine fluids than with nonmarine fluids, for nonmarine fluids was powerful enough to affect bioclasts but powerless to affect micritic matrix.

1. Introduction

Organic reef carbonate rocks are an important component of the carbonate sedimentary system. Oil and gas exploration and development in China and elsewhere have demonstrated that reef facies tend to give rise to large- and medium-sized oil and gas fields and that they also contain rich solid mineral resources [1–6]. Since the late 1970s, with the exploration and development of reef oil and gas reservoirs in south China, research on Permian reefs in that area has made great progress, and there are many relevant research achievements. At the beginning of the 21st century, with the exploration and development of Ordovician carbonate reservoirs in the Tarim Basin, major breakthroughs were made in research on Ordovician reefs in the basin [7–14]. However, the research progress of the Permian reefs in the Tarim Basin is quite slow. In the late 1980s, geologists from the Jianghan Petroleum Institute found abundant Carboniferous-Permian reefs in Pishan, Yecheng, and Shache counties in the southwest margin of the Tarim Basin. They focused on the Permian Keziliqiman Formation reef of the Sangzhu section near Keziliqiman village, Sangzhu Township, Pishan County, to describe its biological characteristics, microfacies, and petroleum geological significance [15, 16] Some scholars have also taken an interest in Permian reef limestone in the northwest margin of the Tarim Basin. However, on the whole, there are few research results on Permian reefs in and around the Tarim Basin. Moreover, the few research results are mostly macrogeological, and studies on reef diagenesis and evolution model are relatively lacking. Therefore, an in-depth study of Carboniferous-Permian reefs in the southwest Tarim Basin is of great significance: it will contribute to the examination of the paleoclimate and paleoenvironment and to the oil and gas exploration of Permian reefs in this area. On the basis of previous research and outcrop observations and laboratory analysis, this study analyzes in detail the development characteristics (including paleontology and reef facies) of the Keziliqiman Formation in the Sangzhu section. Then, we propose a reef evolution model and discuss tentatively the diagenesis types, which we hope can provide a useful reference for in-depth research on Permian organic reefs in the southwest Tarim Basin.

2. Regional Geological Overview

The southwest Tarim depression is located in the southwest margin of the Tarim Basin (Figure 1(a)). From the Early Carboniferous, transgression initiated from west to east in the southwest Tarim Basin, which was then a neritic shelf. In the Middle-Late Carboniferous, carbonate platform facies began to develop on the basis of the original mixed shelf. In the Late Carboniferous-early Early Permian when transgression reached the maximum range, the southwest Tarim Basin inclined from east to west in terms of paleogeomorphology. Meanwhile, the carbonate platform also reached the maximal scale in this area. In the middle-late Early Permian when seawater started to retreat, this region began to assume transitional marine-continental facies. In the Late Permian when seawater completely retreated, it entered a stage of pure continental facies sedimentation. Overall, the Carboniferous-Permian witnessed a complete "transgression-regression" cycle in the southwest Tarim Basin.

The southwest Tarim depression is a first-order structural unit in Tarim Basin, with an area of about $12 \times 104\,km^2$. It is bounded by the Serikbuya-Mazartag fault in the northeast and the piedmont Kalpintag fault in south Tianshan Mountains in the north and adjoined by the Tiekelike uplift on the northern edge of Kunlun Mountain structural belt [12]. According to the structural zoning, the southwest Tarim depression can be divided into such secondary structural units as piedmont thrust nappe structural belts, Khotan-Kashgar depression belt, and Markit Slope (Figure 1(b)).

In terms of stratigraphy, the Carboniferous-Permian strata are widely exposed in the southwest Tarim depression. While they are relatively complete in the west, the lower Carboniferous is mostly missing in the east, and thus, the upper Carboniferous is often in unconformable contact with the Devonian.

In terms of lithology, the Carboniferous System in the southwest Tarim depression is composed dominantly of marine carbonate rocks, with some littoral clasolite. The lithology of the lower Permian is also typically marine carbonate rocks, and that of the Middle-Upper Permian is mainly transitional marine-continental facies and continental facies sediments. In short, the vertical and horizontal lithological changes of the Carboniferous-Permian in the southwest Tarim depression generally reflect that the southwest Tarim region was a complete transgression (from west to East)-regression (from east to West) cycle in the Carboniferous-Permian period. The Carboniferous-Permian carbonate rocks were mainly developed in the carbonate rocks of Azigan Formation (C_2), Tahaqi Formation (C_2-P_1), and Keziliqiman Formation (P_1). They are important reservoir systems of Carboniferous-Permian in southwest Tarim depression. Among them, the Keziliqiman Formation is located top of the other two, with the largest thickness, ranging from 243 m to 550 m, and it tends to become thinner from West to East [13, 14, 17, 18].

The rock samples of the Early Permian Keziliqiman Formation in the Sangzhu Section were put under carbon-oxygen isotope tests (Figure 2), and results show that $\delta^{13}C$ value rises from negative to positive from bottom up, until it reaches the maximum at the position of Keziliqiman reef. Then, at the reef cap, it drops rapidly again. Considering that $\delta^{13}C$ tends to positively correlate with the rise and fall of sea level [15, 16, 19, 20], it can be inferred that when the Keziliqiman reef in Sangzhu developed, the southwest Tarim Basin was undergoing a rise of sea level in the Late Carboniferous Early Permian. While the reef was growing, reef building organisms were flourishing; when they died and were buried quickly, they absorbed a large amount of ^{12}C, resulting in the relative enrichment of ^{13}C in seawater. However, in the exposed part of the reef cap, the value of $\delta^{13}C$ rapidly drops to 0.119‰, which is consistent with the carbon isotope characteristics of tidal flat dolomite [21]. This suggests that when the reef cap was developing, the climate became hot and dry in the Sanzhu area, leading to the sharp decline of the sea level and the eventual disappearance of the reef.

3. Materials and Methods

This study is based on systematic field observations and measurements of the Permian stratum of >1000 m thick and on sampling and photography of reef intervals in the Sangzhu section of Pishan County. Different reef samples were taken for different experimental analyses such as conventional/cast thin section analysis, cathodoluminescence (CL), and carbon-oxygen isotopes. Ninety-six thin sections were impregnated with Canadian balsam and 52 with blue epoxy resin, and they were marked with alizarin red and potassium ferricyanide solution to distinguish calcite and dolomite. At the same time, considering that the growth and development of reefs are closely related to sea levels, this study took 13 coral reef samples for carbon-oxygen isotope testing, and its purpose is to analyze sea-level changes. In the sampling process, places that were strongly transformed by dissolution, cementation, and tectonism were shunned, and rocks with a high degree of recrystallization were also ruled out as far as possible, to ensure the usability of the samples. The samples were sent to the Experimental Teaching Center of Oil and Gas Geology and Exploration of Southwest Petroleum University, where examination was conducted with an Isoprime100 isotope mass spectrometer. In order to analyze the diagenesis of the reef, some thin sections were also examined with CL and electron probe micro-analysis (EPMA). The EPMA was carried out on a JXA-8230 electron probe in the laboratory of School of Geoscience and Technology, Southwest Petroleum University. The CL was conducted on the CL8200 MK5 microscope in the State Key Laboratory of Oil and Gas Reservoir Geology and Exploitation, Southwest Petroleum University; the ambient temperature was 25°C, the experimental vacuum of the CL instrument is 0.3 PA, the beam voltage is 8.0 kV, and the beam current is 6000 μA, and the exposure time is 1.5 s.

4. Results

4.1. Petrographic Types of the Reef. Classification of carbonate rocks is the basis of and important reference for the study of their lithofacies paleogeography. Based on Dunham's

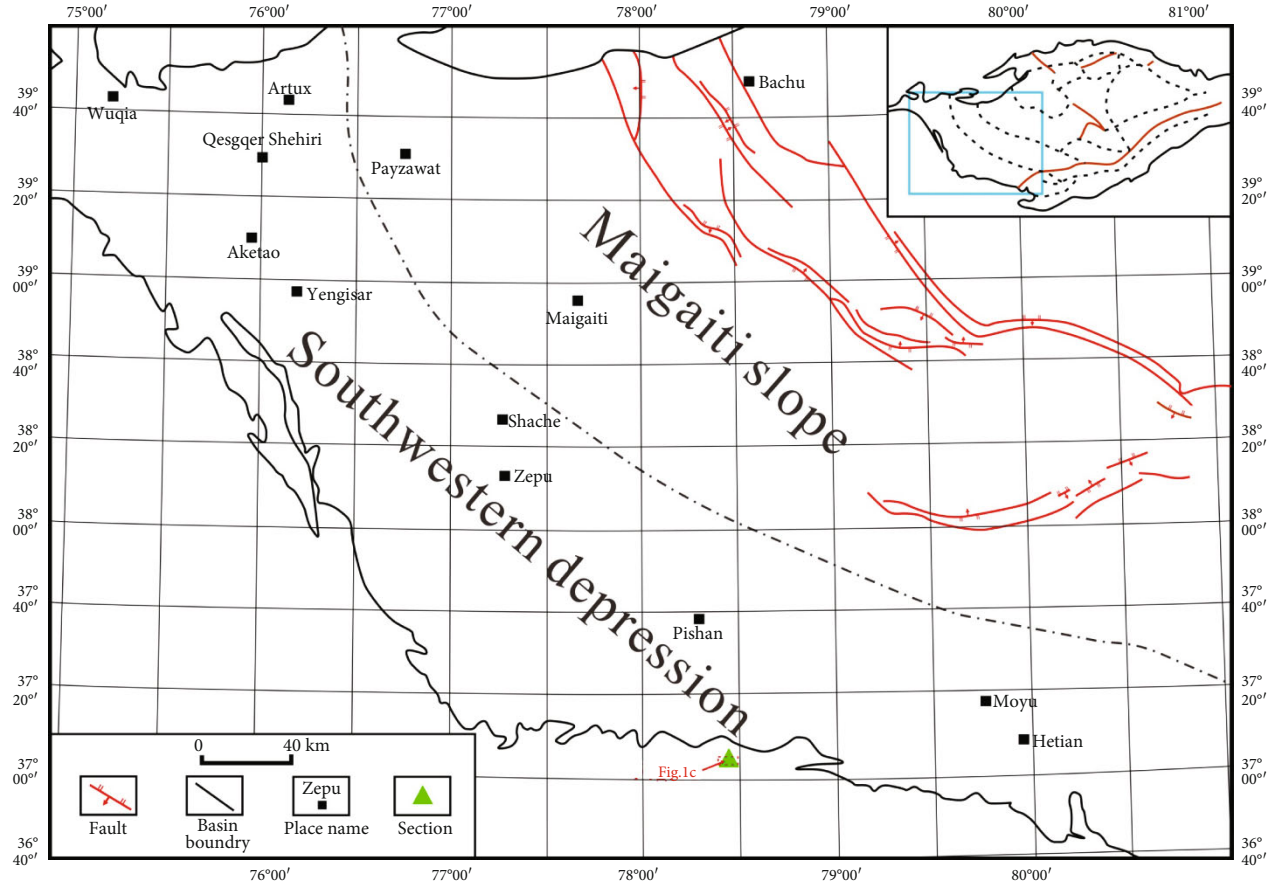

Figure 1: Location plan of the southwest margin of the Tarim Basin, Northwest China. (a) Plan of the Early Permian sedimentary facies in the southwest Tarim Basin. (b) Location plan of the reef.

classification scheme of carbonate rocks [22] and considering the actual status of outcrops, this paper divides the rocks of the Keziliqiman reef into sponge bafflestone, coral framestone, bioclastic grainstone, packstone, mudstone, and micritic-powdery dolomite (Figure 3).

4.1.1. Sponge Bafflestone. Mainly found in the lower zone of the reef core, it developed from the sediments captured through the barring action of *Colospongia*. Because the sponges were mostly strips (10-15 cm in the longitudinal section) and distributed in clusters on the plane, they slowed down the flow rate of water, creating an environment for passing objects to deposit. It is worth noting that the spaces between individual sponges are typically filled by micrite, with little of other types of bioclasts, indicating that the hydrodynamic force of the environment in which they were

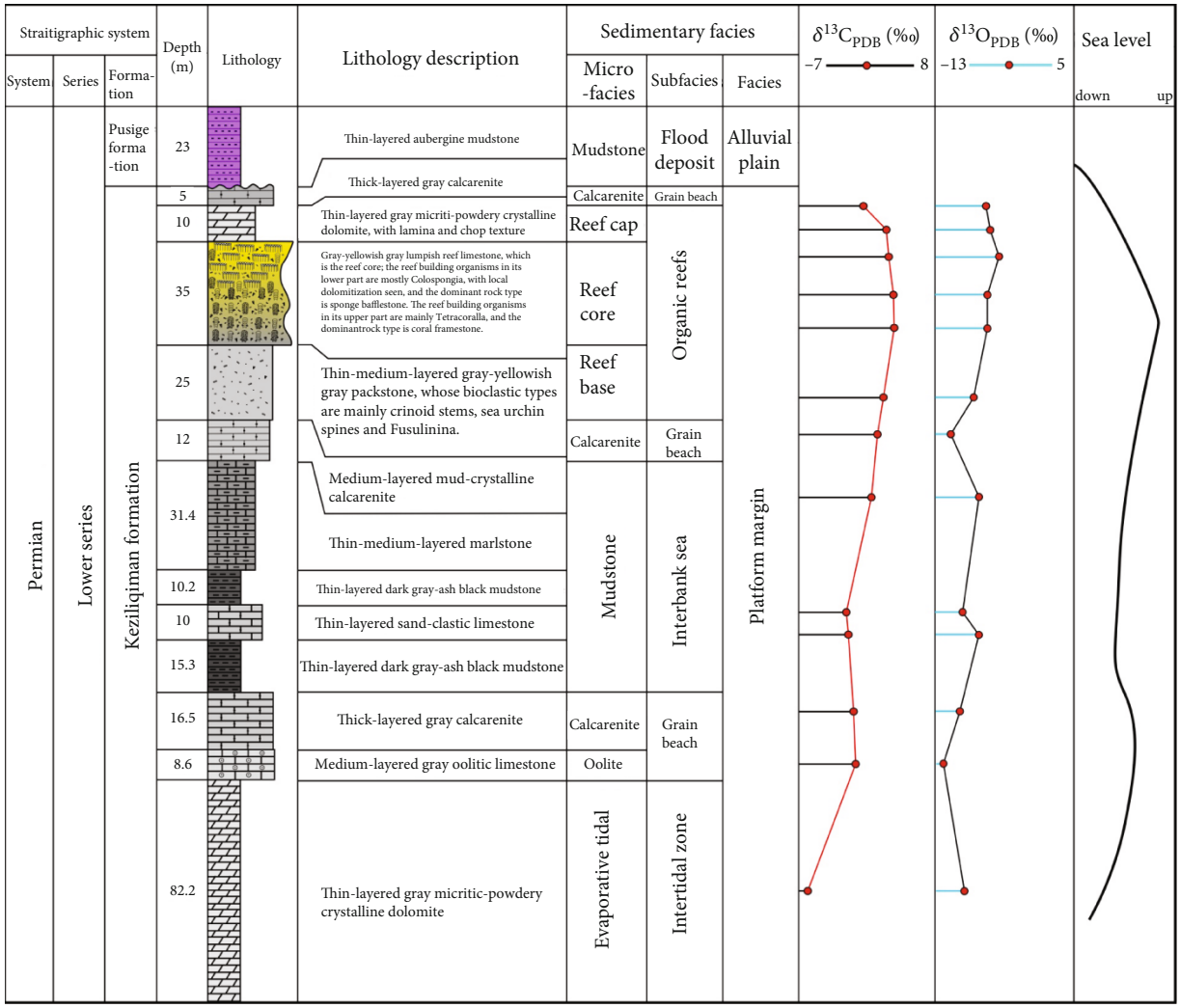

Figure 2: A lithologic histogram of the Keziliqiman Formation in the Sangzhu section.

deposited was relatively weak. In addition, some sponges have been dolomitized locally or entirely, but their contours are still visible (Figure 3(b)).

4.1.2. Coral Framestone. They are mainly distributed in the upper zone of the reef core. During sedimentation, the lumpy colonial Tetracoralla, which grew in situ and were capable of building hard grids, constituted the framework of this type of rock. Microscopically, the spaces between frameworks of these corals are typically filled by accessory reef organisms such as crinoid stems, Fusulinina and Bryozoans (Figure 3(c)), with little marl content. In addition, the holes of the coral framework are basically filled by sparry calcite. These factors make the reef strong enough to resist waves; and they also suggest that there was a strong hydrodynamic force in the environment in which it was deposited.

4.1.3. Biograined Limestone. Typically, gray-grayish and with a structure supported by bioclasts, it is mainly found in the reef front. The bioclasts, which are mainly of Fusulinina, brachiopods, and echinoderms (Figure 4(e)), account for more than 90% in content. A small number of solitary corals can be seen locally, and the content of micrite is very low. Due to the action of waves, the distribution of bioclasts is often irregular (Figure 3(e)).

4.1.4. Packstone. Typically gray-ash gray and with a structure mainly supported by marl and locally supported by bioclasts, this type of rock is generally seen at the reef base and locally at the back reef (Figure 3(a)). Bioclasts of crinoid stems, brachiopods, Fusulinina, etc. amount to 40%-50% in content. The spaces between the particles and coelomic cavities are often filled with marl (micritic matrix), indicating that there was a weak hydrodynamic force in the deposition period.

4.1.5. Mudstone. Typically, ash black-black and with micritic structure and good stratification (Figure 3(d)), it is mainly found in the low-energy environment of the back reef zone. Under the microscope, the micritic matrix is locally microcrystallized. The content of bioclasts is small, and relatively complete bioclasts of bryozoans, brachiopods, crustaceans, and echinoderms are occasionally seen under the microscope, indicating that the hydrodynamic force was weak. The overall

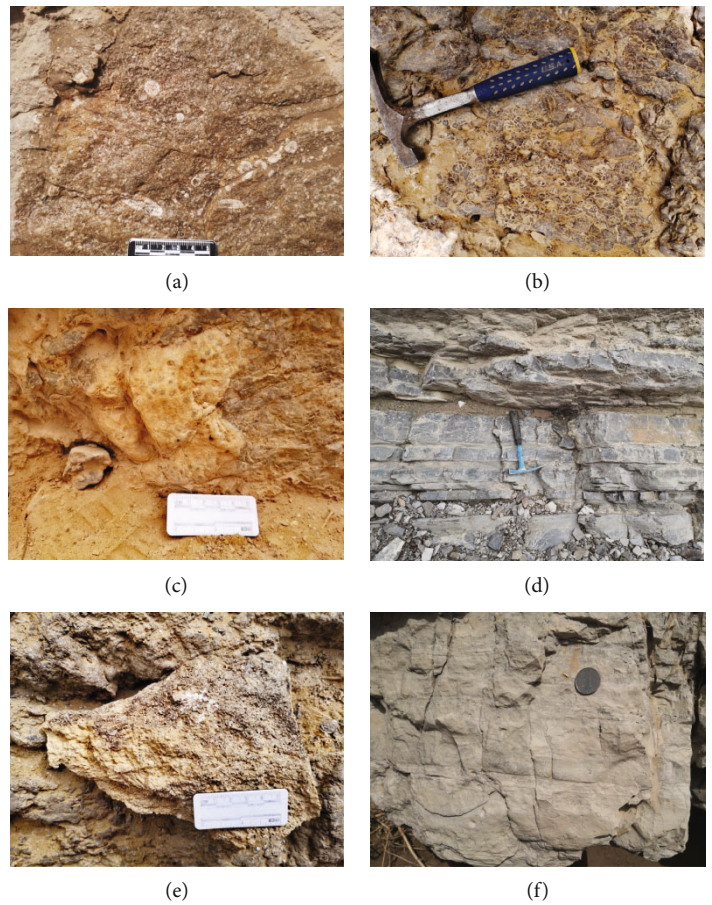

Figure 3: Types of reef limestone in Keziliqiman Formation. (a) Packstone in the reef base, with echinoderms as the main bioclastic type. (b) *Colospongia* bafflestone in the reef core, with most of the sponges dolomitized. (c) Coral framestone in the upper zone of the reef core, with colonial *Tetracoralla* visible. (d) Ash black micrite in the back reef, with good stratification. (e) Bioclastic grainstone in the front reef, with dissolution pores visible. (f) Micritic-powdery dolomite in the reef cap.

structure of the rock is compact, with strong cementation and poor reservoir performance.

4.1.6. Micritic-Powdery Dolomite. Typically, ash gray-grayish, with micritic-powdery structure, it is mainly found in the reef cap zone. Algal lamina are relatively well developed, and dissolved pores and chop texture can be seen locally (Figure 3(f)).

Different rock types are important for determining the microfacies of reefs. Among them, sponge barrier rocks and coral skeleton rocks are found in the lower and upper parts of the reef core, respectively. Argillaceous-pink dolomite appears in the reef cap, indicating that the biological reef has died out. The biological granular limestone mainly indicates the high-energy environment in front of the reef. The crystalline limestone indicates the postreef low-energy environment, and the bioclastic granular limestone is mainly found in the reef base. Based on this, a cross-sectional view of the reef microfacies structure was drawn (Figure 4).

4.2. Paleontological Features of the Reefs

4.2.1. Types of Reef-Building Organisms

(1) Sponge. They were mostly Colospongia of Demospongiae. Vertically, their chambers were often spherical or annular, with a diameter of 1.5-3.5 cm (Figure 5(b)). The stacking pattern of chambers from top to bottom gives sponges (4.5-20 cm long) the shape of beads of a string. These sponges, 4.5-20 cm long, occurred mostly in crowded clusters (Figure 5(a)), with a few solitaries. On the cross section, a clear "central cavity" of about 1 cm in diameter can be seen. In general, *Colospongia* are rather intact in shape, though dolomitization also occurred in some of them (Figures 5(a)–5(c)). Microscopically, even the dolomitized ones have desirable shapes and microstructures. And the micropores in the outer wall of the chamber and the residual grid-like skeletal structure inside the chamber are still vaguely visible (Figure 5(d)). In addition, a small number of *Subascosymplegma* can be discerned, whose chambers, often crescent shaped, are vertically stacked into something like a plank (Figure 5(e)).

Sponges are mainly distributed in the lower zone of the reef core and are the main building organisms in the early stage. C*olospongia* can also be seen locally in the upper zone of the reef core, but they are not dominant. Besides, a small number of sponges can be seen in the back reef.

(2) Coral. Small in number and typically as lumpish compounds (with a few solitary ones), they are mainly distributed

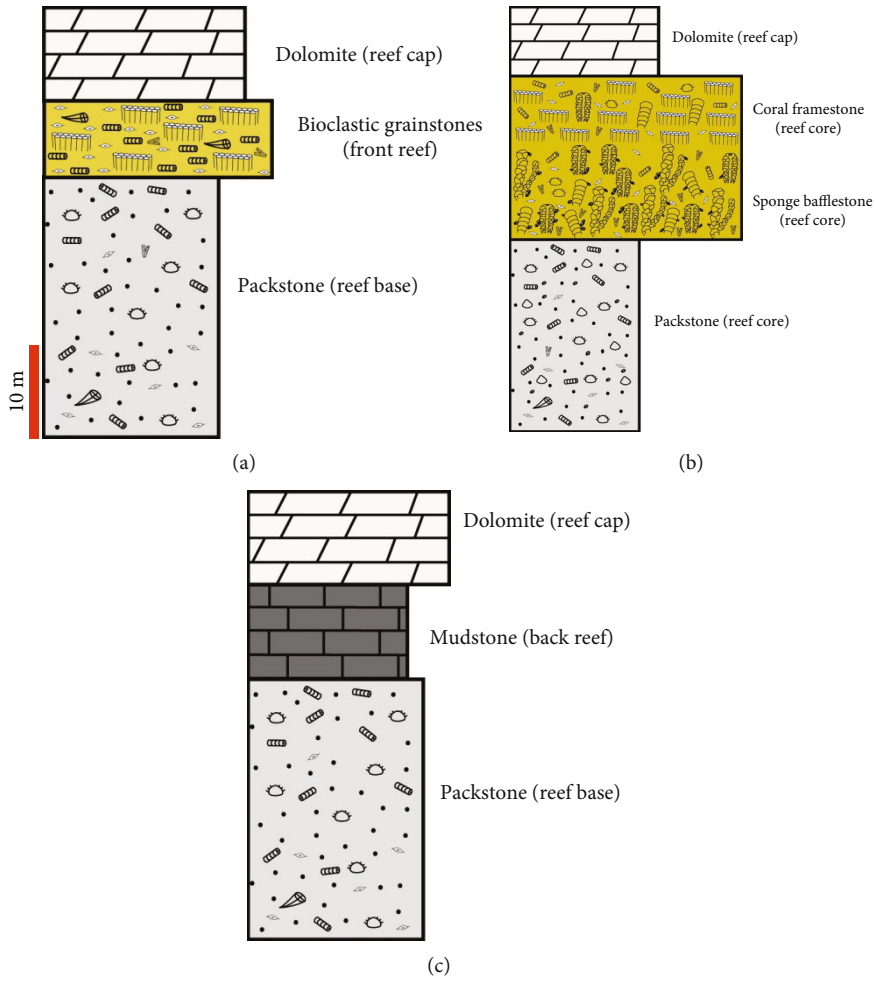

Figure 4: Reef microfacies structure of Keziliqiman Formation in Sangzhu section.

in the upper zone of the reef core. In terms of species, *Kepingophyllidae*, a member of Tetracoralla, are dominant. Growing perpendicularly to and along the bed, and sometimes symbiotic with *Colospongia*, they measured approximately 10-50 cm in height. Among the compounds, individuals are often in polygonal mosaic contact horizontally (Figures 6(a)–6(c)).

Microscopically, the septa of the individual are quite developed, with regular and herringbone dissepiments within them. In the center of the individual is an intricate axial structure, which, in a cross section, looks like that of a "walnut" almost halved by the median plate. Some individuals have simple axes or compact middle axes. Foam belts are quite well developed. Most of the septa are minor, while some are tertiary. The initial ends of the septa often extend unevenly within the foam belts.

In addition, *Kepingophyllidae* have distinctive theca. Wu Wangshi et al. hold that, unlike most *Tetracoralla*, *Kepingophyllidae* have no thin epithelium of guard (full theca) on the outermost side of the theca and hence no outer wall of guard. Instead, three types of theca (false theca) developed: spinous, lamellar or scaly, and septal, which are peculiar to the wall structure of *Kepingophyllidae*. In the compound *Kepingophyllidae* that we found, individuals are mostly separated by false theca. Among them, compound corals with well-developed septa mostly have septum-like theca due to the interpenetration and thickening of septa (Figure 6(d)), but other types of false theca (e.g., spinous) can also be seen between individuals. The distribution of false theca types shows a certain degree of heterogeneity.

Nondissepimented individuals (Figures 6(e) and 6(g)) can also be seen at the front reef, with a nearly circular cross section and a diameter of approximately 1-2 cm. According to previous studies, these corallites often occurred in deep-water, oxygen-poor, and muddy hydrostatic environment or cold-water environment.

(3) Bryozoans. The types of bryozoans are diverse. Microscopically, *Fenestella*, *Polypora*, *Chabdomesid*, and *Ptilodictyna* (all four are *Cryptostomata*), *Cerioporoid* of *Cyclostomata*, and *Fistulipora* of *Cystoporata* can be identified. Among them, *Fenestella* are the most common, and their reticular zoaria can be discerned under the microscope (Figures 7(a) and 7(b)). The fenestrule is rectangular to oval, and two rows of zooecia can be clearly seen on both sides. The zooecia are

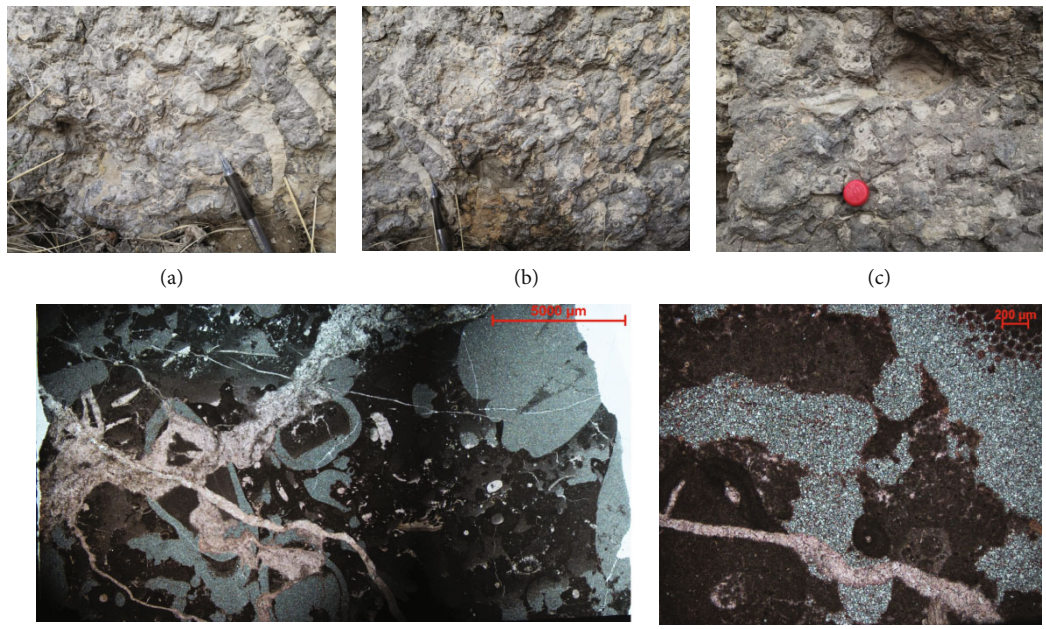

Figure 5: *Colospongia*. (a)–(c) are outcrop photos of *Colospongia*. (d) and (e) are photomicrographs of *Colospongia*.

mostly oval or near round, and a few are approximately pentagonal and rhombic. The grid zoarium is often connected by many horizontal forks, most of which also have zooecia. Filament-lamellar sparry calcite can be seen around some *Fenestella*. These synsedimentary seafloor cements were often the hard ground on which bryozoans grew. In the low-energy back reef zone, the zooecia of some *Fenestella* are often connected with each other to form a "necklace" structure (sometimes with "forks," Figure 7(d)). In addition, *Ptilodictyina* with bilayer symmetrical zoaria (Figure 7(e)) and *Polypora* with forks are also common (Figure 7(c)).

In the process of erect growth, *Cryptostoma*'s reticular zoaria collected clay-graded carbonate sediments, while their fenestrules and zooecia were easily filled by marl, thus forming bafflestone. Bryozoans were mainly seen in the front reef zone and also in the base and back, often symbiotic with sea urchins and crinoids. Because their calcareous zoaria were fragile and susceptible to wave impact, most bryozoans in the front reef were present in the form of fragments. The zoaria in the mudstone of the back reef were mostly well preserved.

(4) Cyanobacteria. Cyanobacteria are also called blue-green algae, and they have diverse morphological characteristics. Under the microscope, they often appear in the form of micritic cakes or globular grains of different sizes and are densely distributed (Figure 8(a)). Some of them take the shape of irregular lamellar cladded filaments interlayered with microcrystalline carbonate, giving rise to algal boundstones (Figures 8(b) and 8(c)). Close to the front reef, nodular structures (oncoids, Figure 8(d)) wrapped by *Cyanobacteria* can also be seen locally.

(5) Tubiphytes. They can be seen in large numbers in the reef core. There was controversy over their categorization as *Cyanobacteria*, sponges, or bryozoans. Recent studies assume that they are *Cyanophyta* (*Cyanobacteria*)-*Foraminifera* symbionts, commonly found among various bioclastic particles. Their cross sections typically have concentric rings, with a round cavity in the center (a common feature of *Tubiphyte*). Nevertheless, most of them take the shape of strips, leaves, or even amorphous aggregates with two or more cavities (Figure 9(a) and 10). They often adhere to and colonize the zoaria of bioclasts of *Colospongia*, bryozoans, and echinoderms.

In short, the building organisms of the Keziliqiman reef were dominantly *Colospongia*, followed by *Kepingophyllidae*, and *Bryozoans* of *Cryptostomata* are also common; all of them contributed to the framing of the reef. As they were able to bar marl and bioclasts, which in turn were bound by *Tubiphytes* and *Cyanobacteria*, the reef grew to be resistant to waves to some extent. However, because *Colospongia* and bryozoans had poor wave resistance while colonial *Tetracoralla*, which had rather strong wave resistance, were small in number, the Keziliqiman reef can be classified into a "stratigraphic reef" in a broad sense. This is similar to the Permian reefs in South China.

4.2.2. Types of Accessory Reef Organisms. In the Permian Sangzhu reef, there were various types of accessory reef organisms: *Fusulinina*, gastropods, Langella, echinoderms, etc. Among them, *Fusulinina*, as a typical Carboniferous-Permian fossil, were important accessory organisms of the reef. In reef thin sections of the Keziliqiman Formation, diverse species can be identified: *Profusulinella*, *Parafusulina*, *Triticites*, *Verbeekinidea*, *Schwagerina*, etc., with *Parafusulina* and *Schwagerina* as the most common (Figures 8(a) and 8(b)). The shells of gastropods are mainly conical and dextral. *Echinoderms* are mainly crinoids and sea urchins. Microscopically, they mostly occur in the form of osseous lamella, and sea urchin spines can be seen occasionally.

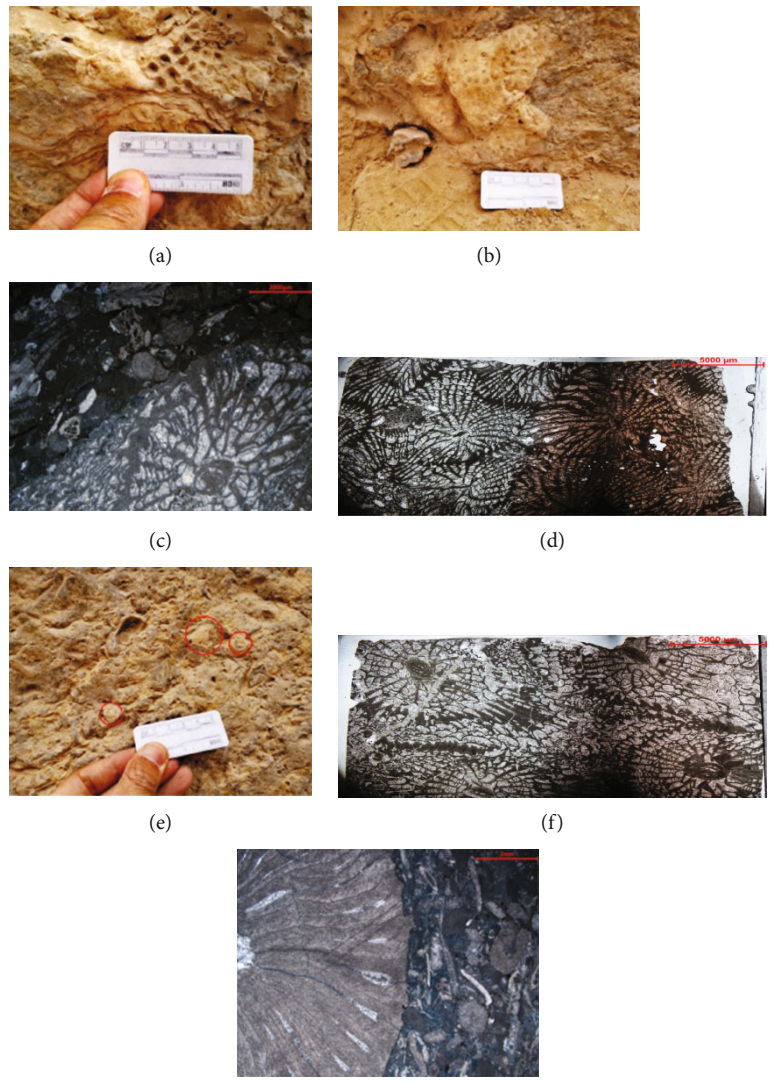

(a) (b) (c) (d) (e) (f) (g)

Figure 6: Corals. (a) and (b) are outcrop photos of *Kepingophyllidae*. (c), (d), and (f) are photomicrographs of Kepingophyllidae. In (d), individual corals are separated by septal theca (indicated in red circles); in (f), individual corals are separated by squamotheca (indicated in yellow circles) and brambly-theca (indicated in red boxes). (e) and (g) are outcrop (indicated in red circles) and microscopic photos of individual corals.

4.3. Features of Reef Facies

4.3.1. Reef Base. Approximately 28 m thick and continuous and stable horizontally, it is the bed on which the reef grew. It consists mostly of packstone (bioclastic shoal), with local oolitic limestone (oolitic shoal, partially dolomitized). An abundance of crinoid stems is seen in outcrops, while a large number of sea urchin stems is discerned under the microscope. Sea urchin stems are generally <0.5 cm in diameter, accounting for 70%-80% of the total bioclasts. Other bioclasts (bivalves, *Fusulinina*, ostracods, etc.) take up 20%-30% in content. Microscopically, the original coelomic pores of these organisms are often filled by micrite (Figure 11), indicating that the hydrodynamic force when the reef base was taking shape was not strong enough to conduct winnowing. Some dissolution pores can be seen locally. Its bottom is in conformable contact with calcarenite (calcarenitic shoal).

4.3.2. Reef Core. Approximately 20 m thick, it is the main structure of the reef. The building organisms include *Colospongia*, *Tetracoralla*, *Bryozoans*, and *Cyanobacteria*. Accessory organisms are *Lamellibranchia*, gastropods, echinoderms, and other benthos. The biological types in the lower zone of the core are not as diverse, with *Colospongia* predominant and a small number of bryozoans and *Tubiphytes* adhering to them (Figure 10). The spaces between individual sponges are often filled by marl, with few accessory organisms. The building organisms in the upper zone are relatively diverse, including *Colospongia*, *Kepingophyllidae*, and bryozoans. Among them, corals often occurred along the bed. Microscopically, around the colonial corals can be seen an accumulation of bioclasts of echinoderms, *Fusulinina* and bryozoans in large numbers, and sponges in small numbers.

The change in reef-building organism types and the external morphology of these organisms are indicators of

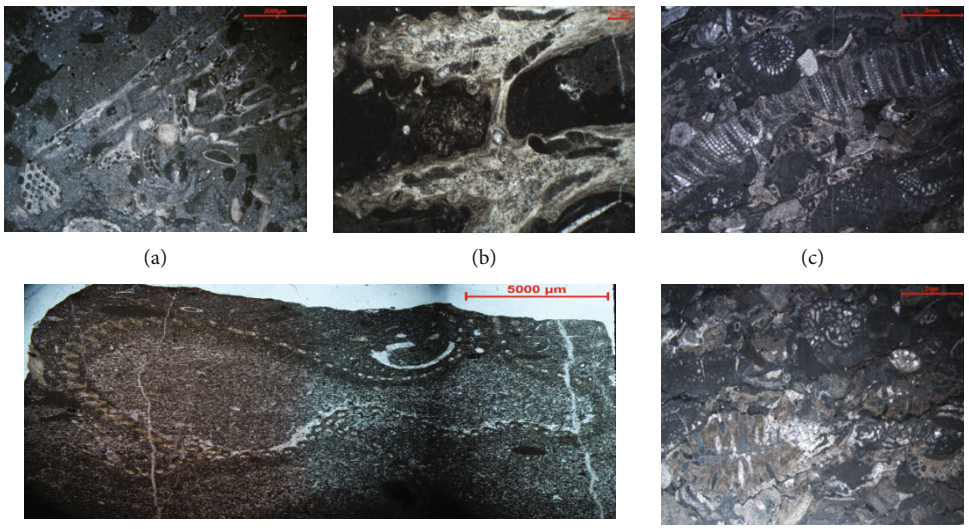

Figure 7: *Bryozoans*. (a) *Fenestella*, with distinct fenestrule and zooecia and accessory organisms such as *Fusulinina*; (b) *Fenestella*, with distinct fenestrule and zooecia; (c) the *Polypora* fragments, connected by filament calcite; (d) *Fenestella*, whose zooecia are connected to form a major "necklace" that forks out into several minor ones; (e) *Ptilodictyina*, with bilayer symmetrical zoaria.

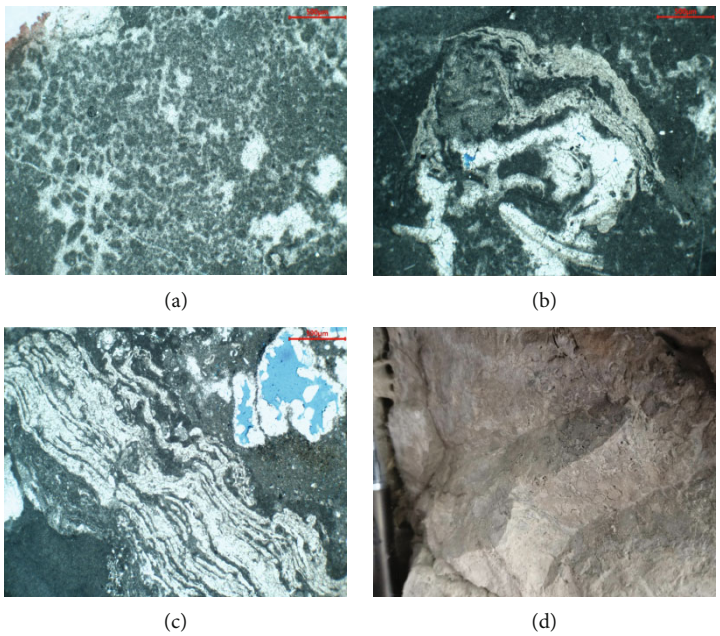

Figure 8: *Cyanobacteria*. (a) Globular *Cyanobacteria* under the single polarizer; (b) lamellar cladding of *Cyanobacteria* interbedded with powdery-fine-crystalline carbonate rocks under the single polarizer; (c) lamellar cladding of *Cyanobacteria* interbedded with powdery-fine-grained carbonate rocks under the single polarizer; (d) oncolitic limestone.

the energy level of the water body in the growth period of the reef. Generally, spherical, lumpish, and stubby organisms tend to live in high-energy shallow environments, while cylindrical and lean organisms tend to dwell in rather quiet environments. In the Keziliqiman Formation reef of the Sangzhu section, most of the *Colospongia* are cylindrical, unadaptable to a high-energy environment; the spaces between individuals are often filled by marl—these two factors suggest that when *Colospongia* were growing, the hydrodynamic force was unable to create waves for winnowing. At this time, the reef was typically a sponge barrier.

Tetracoralla, which tend to occur in high-energy environments, have quite strong wave resistance. They are mostly lumpish compounds, with mosaic contact between individuals. The content of bioclasts around the colonial Tetracoralla is high, and the types of bioclasts are diverse, such as echinoderms, bryozoans, *Fusulinina*, and a small amount of sponge fragments. It can be inferred that colonial Tetracoralla appeared

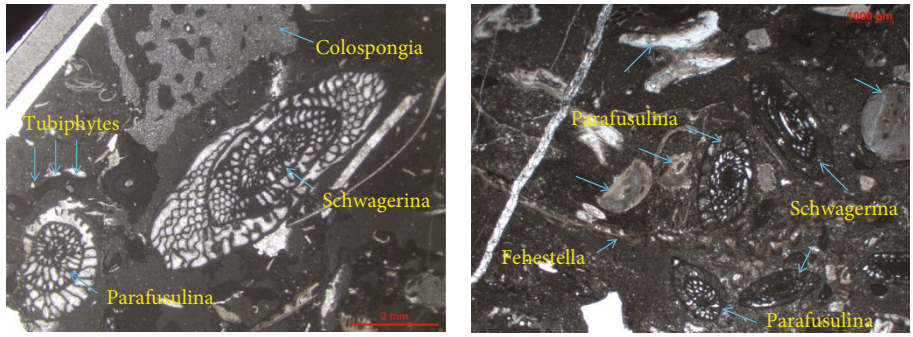

(a) (b)

Figure 9: Types of accessory reef organisms. (a) Rather intact *Schwagerina* (indicated by the yellow arrow) and *Parafusulina* (indicated by the red arrow), symbiotic with *Colospongia* (indicated by blue arrows), among which are accessory *Tubiphytes* (indicated by green arrows); (b) rather intact *Schwagerina* (indicated by yellow arrows) and *Parafusulina* (indicated by red arrows), around which the bioclasts of echinoderms (indicated by blue arrows) and *Fenestella* (indicated by the green arrow) are visible.

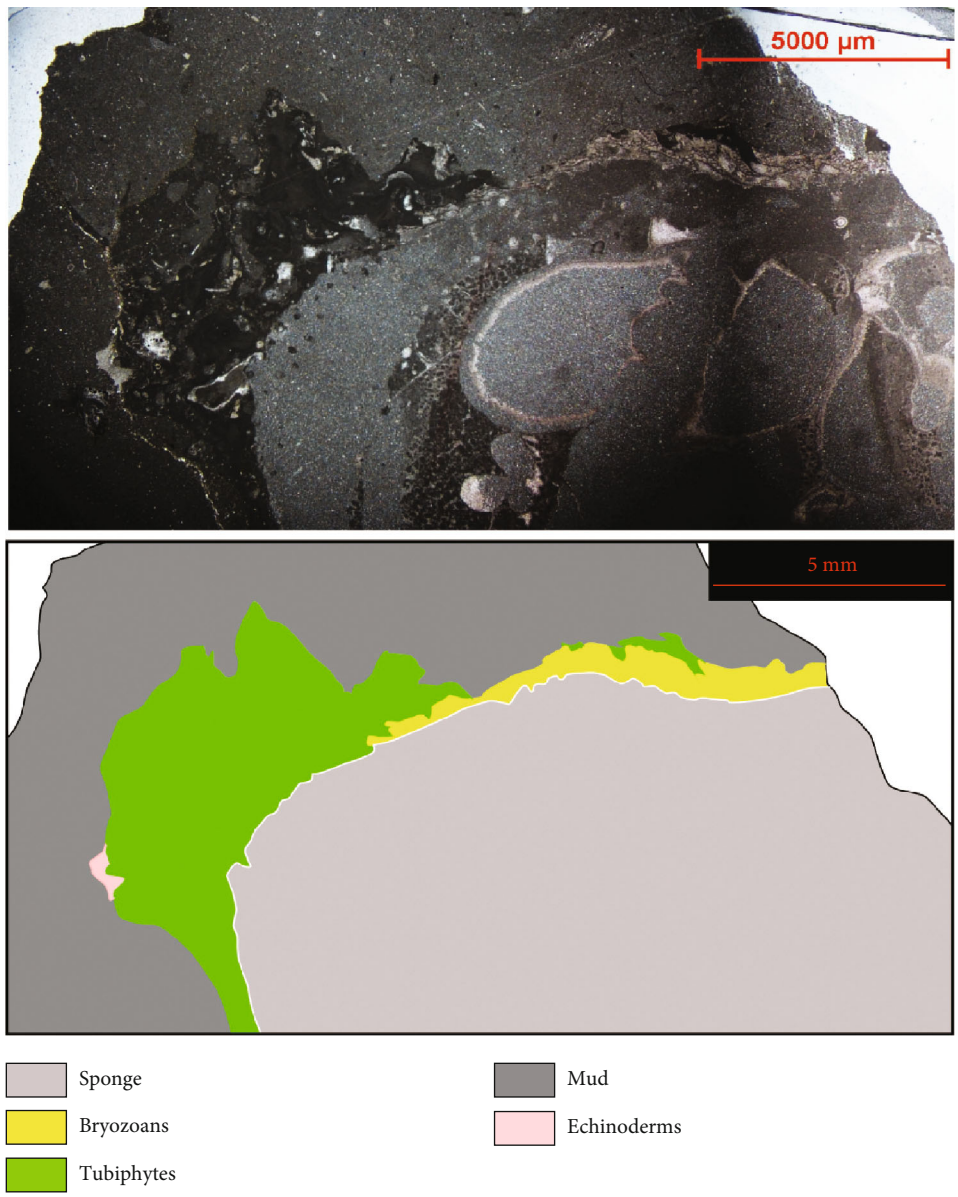

Figure 10: A typical thin section of the lower zone (abundant in Colospongia) of the reef core and color rendering.

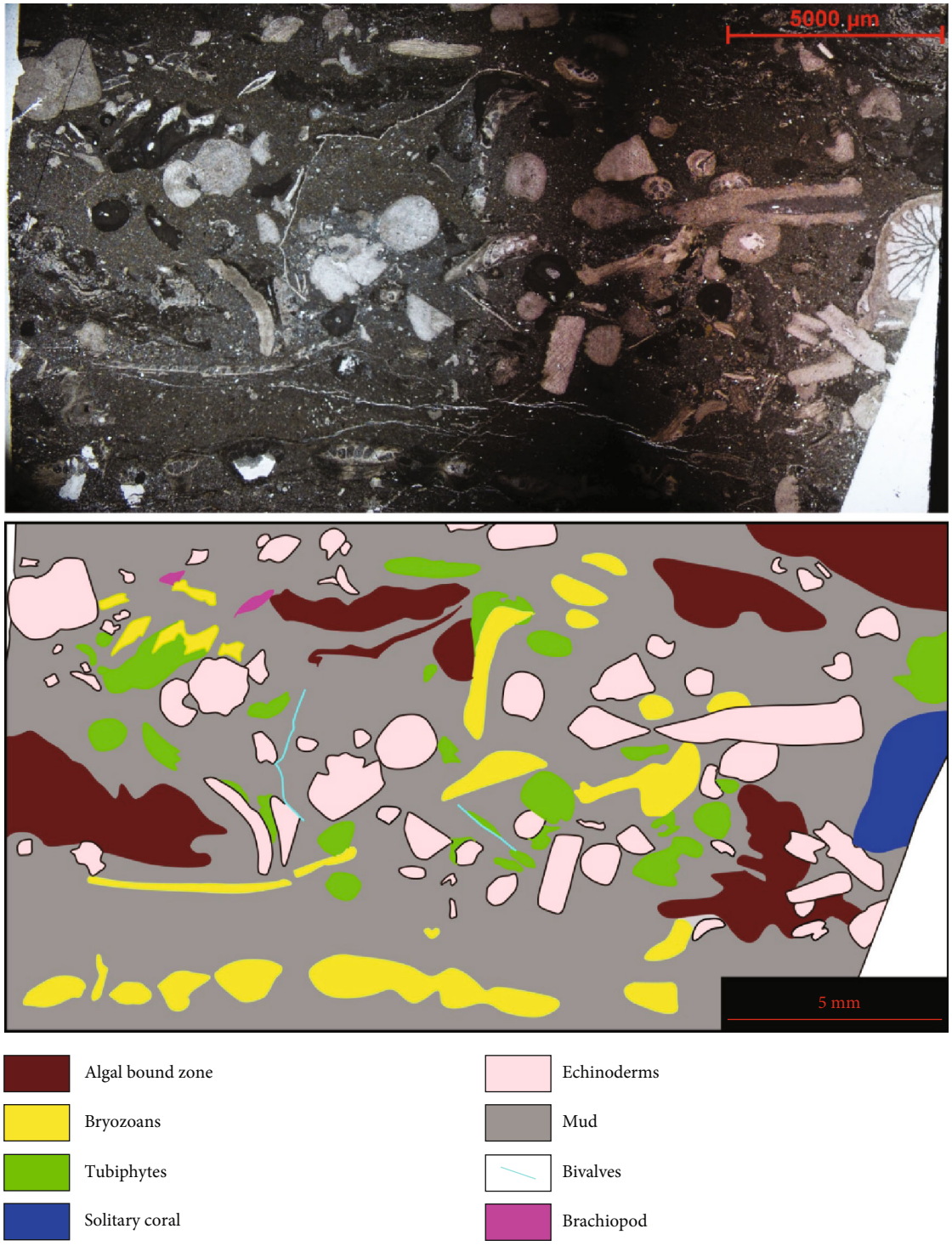

Figure 11: A typical thin section of the reef base and color rendering.

when the water body was relatively turbulent. As the reef depended on the colonial corals for stability, it is defined as a coral framework reef.

4.3.3. Back Reef. Approximately 12 m thick, it developed behind the reef core, with its lower zone in contact with the base and its upper zone in obvious abrupt contact with the cap of thin-layer algal limestone (mostly dolomitized). The lithology is thin-median thick gray mudstone, with good stratification. Echinoderms, bivalves, *Fusulinina*, bryozoans, gastropods, and a small amount of *Colospongia* fossils can be seen in the small amount of bioclasts.

4.3.4. Front Reef. Approximately 8 m thick, it is mostly composed of bioclastic grainstone, with gray-dark gray oncolitic limestone seen locally. Fragments of corals,

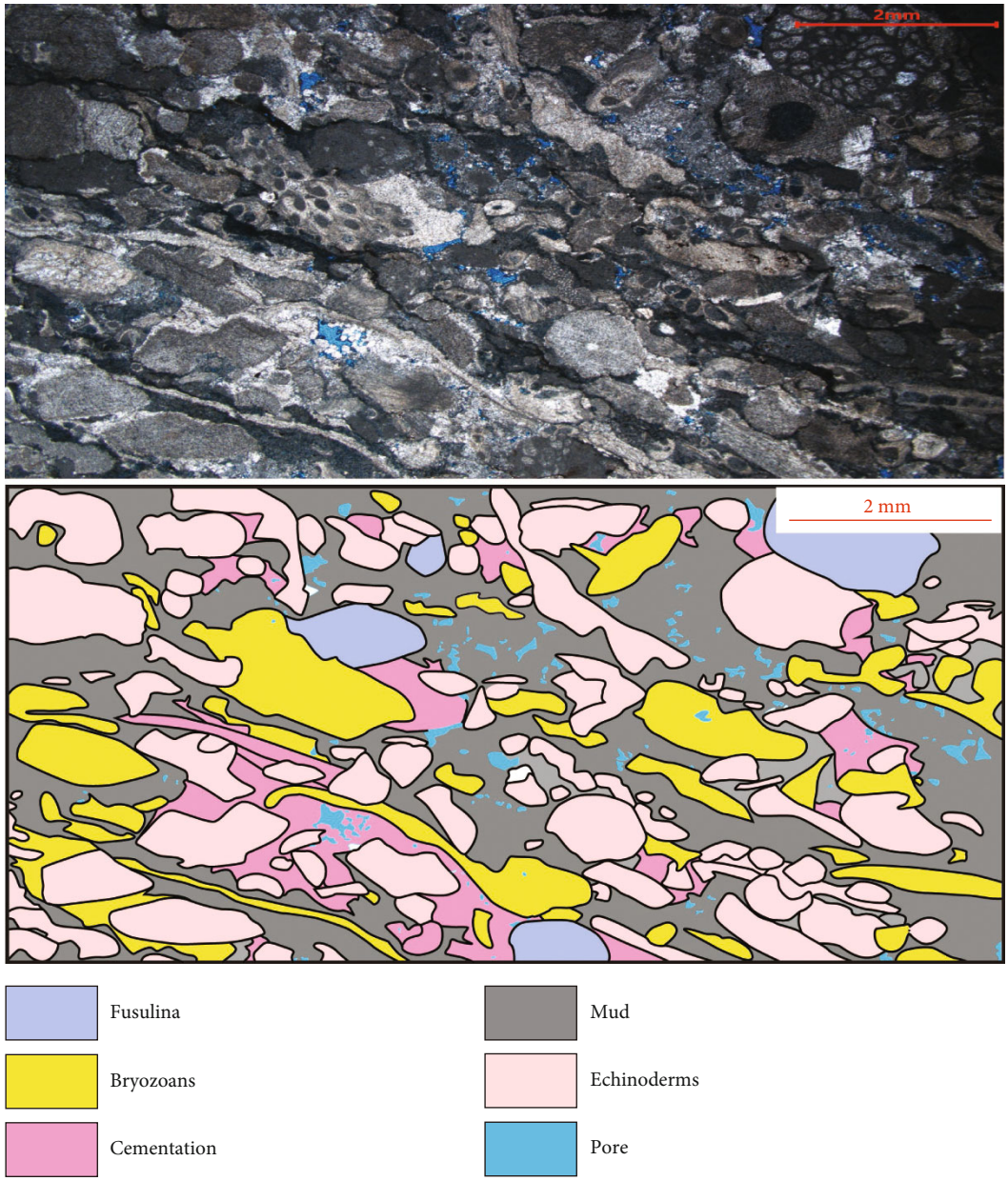

Figure 12: A typical thin section of the front reef and color rendering.

sponges and bryozoans, and fossils of sea crinoid stems and *Fusulinina* are common. Owing to the winnowing action of the strong-energy waves, marl was not easy to deposit, and as a result, bioclasts amount to more than 90% in content. Moreover, under the action of waves, the building and accessory organisms of the front reef tended to be broken, moving along the slope, and then the bioclasts of echinoderms (crinoid stems) and colonial corals accumulated in the form of axes (Figure 12). Because it was exposed to air most of the time and thus subjected to the leaching of atmospheric water, dissolution pores and vugs were rather well developed nearby. A small number of nondissepimented solitary little corals can also be seen along the slope of the front core.

4.3.5. Reef Cap. Approximately 10 m thick and mainly composed of thin-layer algal limestone, it is in transitional contact with the underlying core. There are obvious exposed structures, strong local dolomitization (algal dolomite), and a rather well-developed chop texture—features typical of supratidal deposition.

Based on outcrop observations, the Keziliqiman Formation reef of the Sangzhu section, located east of Keziliger village, Sangzhu township, is distributed generally in a nearly W-E direction. Affected by tectonic movements, the strata are almost vertical, but the reef's overall appearance, spatial distribution, and composition can still be roughly discerned. Its maximum width in the W-E direction is approximately 520 m, while its thickness is approximately 70 m (Figure 1(b)). It is actually a

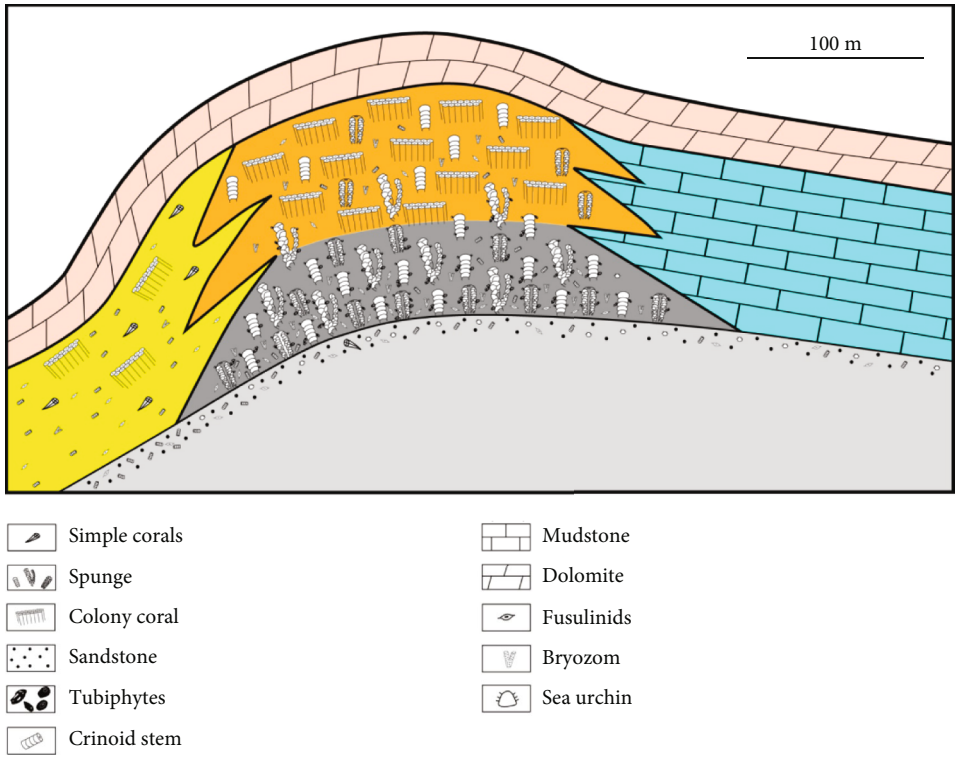

Figure 13: The Keziliqiman organic reef of the Sangzhu section.

point reef on the platform margin. Based on field observations and measurements, a reef profile is drawn (Figure 13).

4.4. Cathodoluminescence and Electron Probe Microanalysis Results. Ever since the Keziliqiman reef took shape, it experienced complex diagenetic processes, including dolomitization, cementation, siliceous metasomatism, and dissolution. As CL technology is one of the most effective means to study diagenesis, diagenetic history, and diagenetic fluid properties of sedimentary rocks, it was applied to test samples from different reef facies of the Keziliqiman reef in Sangzhu section. In order to elaborate on the CL characteristics, the CL intensity of the samples is divided into five scales: very strong, strong, medium, weak, very weak, and nonluminescent. According to previous studies, the CL intensity of carbonate rocks is mainly affected by the contents of Fe and Mn and their ratio. Thereupon, this study conducted electron probe microanalysis (EPMA) of some particles and interstitial materials which demonstrated different CL characteristics; the purpose is to analyze such elements as Fe, Mn, and Sr.

The CL results of 60 samples from the Keziliquiman reef indicate that, generally speaking, the emission in the lower zone of the reef core (with an abundance of *Colospongia*), the reef cap, and the back reef (with mudstone) is relatively weak, while that in the upper zone of the reef core, the front reef (with bioclastic grainstone) and the reef base are relatively strong; thus, there is obvious heterogeneity. In addition, obvious differences are shown in the CL characteristics of samples with different structural compositions. The characteristics are as follows:

(1) Most of the micritic matrix (including micritic envelopes wrapping bioclasts) which has not been transformed by recrystallization (or neomorphism) gives off weak-medium brownish red light, while the micritic matrix which has recrystallized into sparry cement emits very weak brownish red light or no light. The cavities of *Fusulinina*, bryozoans and other organisms are generally filled with micrite, and the CL of the locations that have been recrystallized is generally dim (Figure 14(f)). EPMA results show that the FeO/MnO difference between micrite and recrystallized sparry cement is nearly 10 times. Then, it is clear that recrystallization leads to relative enrichment of Fe (Table 1)

(2) Tubiphytes generally emit strong orange light (Figure 14(b)). *Fusulinina* emit weak-medium orange light (Figure 14(f)). Most brachiopods are nonluminescent (Figure 14(h)). Echinoderm bioclasts vary in luminescence of weak- strong orange (Figures 14(d), 14(f), 14(h), 14(j), and 14(p)). Most sea urchin spines do not emit light, but they emit medium orange light after being locally recrystallized. The calcareous frameworks of Kepingophyllidae generally give off medium-strong orange (stronger than the micritic matrix and granular cement which fill their cavities); the axes of their septa emit quite strong light, the "feathery clasts" on both sides of the septum weak-medium light, while the zones near the axes of the septa no light (Figures 14(f) and 14(j)). Fenestella are generally emitted medium-strong orange light, while

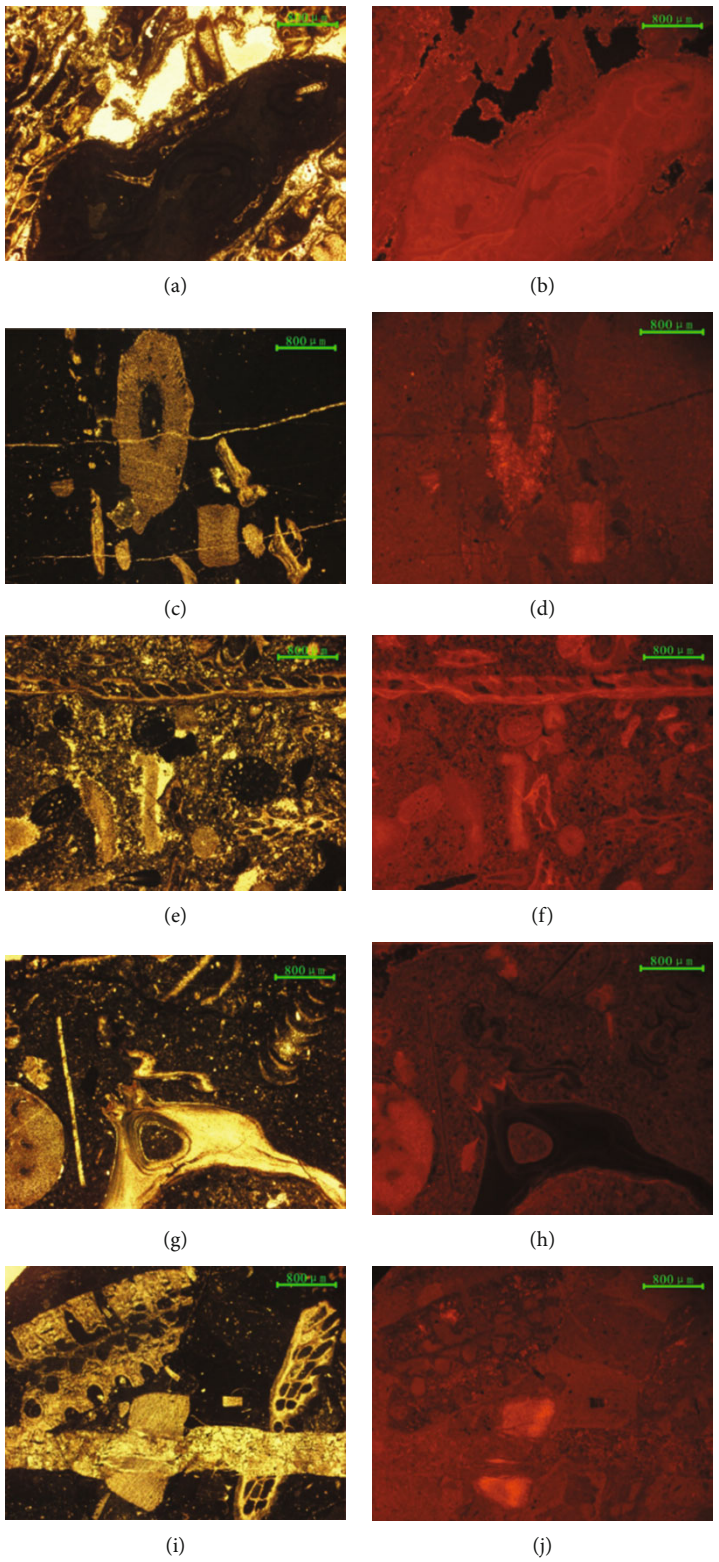

Figure 14: Continued.

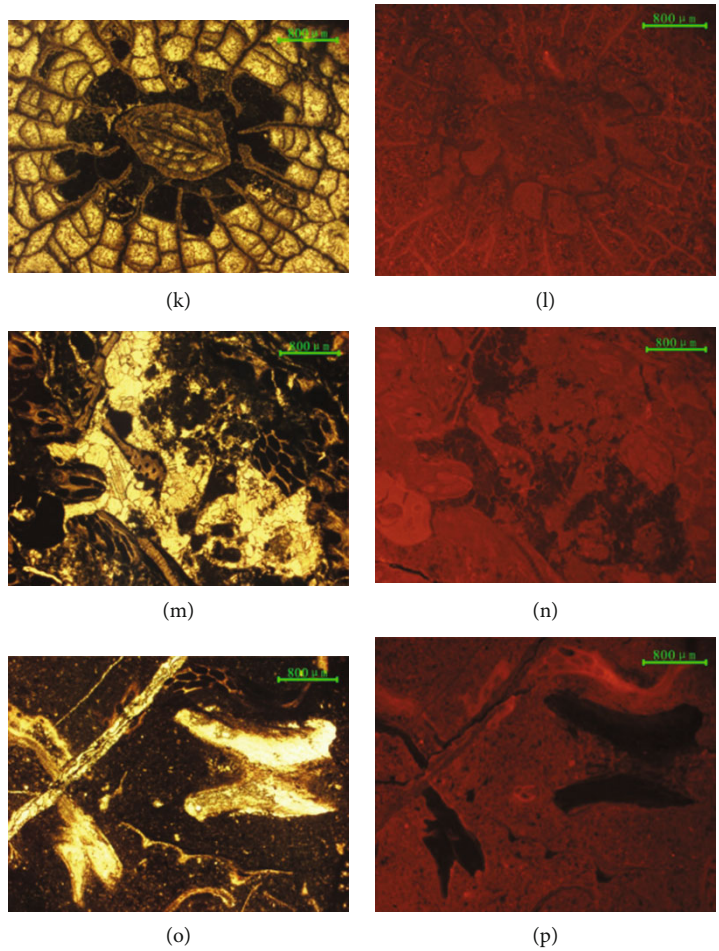

Figure 14: CL characteristics of the reef. In (a) and (b) (reef base), *Tubiphytes*-wrapped bioclasts, with burrow holes visible locally (emitting very weak brownish red light, indicated by blue arrows), produce very weak brownish red light (indicated by green arrows). Dissolution pores are well developed, with calcite cement at the edge; the core part of the cement is nonluminescent while its edge is bright (indicated by yellow arrows). In (c) and (d) (the lower zone of the reef core), sea urchin spines (in oblique sections), cut by fractures (calcite in them does not emit light), can be seen. The upper part of sea urchin spines is nonluminescent, while the lower part sends out medium orange red light (recrystallized). In (e) and (f) (the upper zone of the reef core), the cavities of bryozoans are filled by micritic and sparry cement. The micritic fillings are weakly brownish red (indicated by yellow arrows), and the sparry fillings (recrystallized) very weakly brownish red or non-luminescent (indicated by green arrows). In addition, two generations of cement (indicated by the white arrow) can be seen in the spines. In (g) and (h) (back reef), the clasts of brachiopods and *Colospongia* can be seen, whose bones do not emit light (indicated by yellow arrows). The stem pores of *Brachiopods* and the abdominal cavities of sponges are filled by micrite, and the micrite that fill abdominal cavities of sponges are partially recrystallized, giving off weak red light. In (i) and (j) (back reef), *Ptilodictyina* are symbiotic with echinoderms. *Ptilodictyina* do not radiate light, while echinoderms medium orange light. In (k) and (l), cavities of *Kepingophyllidae* are filled by micrite and spar; the axes of the septa emit orange light of medium-strong intensity; the feathery clasts on both sides of the septa brown red light of weak intensity; the positions near the axes of the septa are basically not luminescent. In (m) and (n) (front reef), intergranular dissolution pores are filled by sparry cement, whose luminescence is dimmer than that of the surrounding micritic matrix. In (o) and (p), *Fenestella* are symbiotic with echinoderms; echinoderms are not luminescent, while *Fenestella* bright red.

Ptilodictyina generally give off weak brownish red, or no light (Figures 14(f), 14(j), 14(i), and 14(p))

(3) The extended edges of some echinoderms give off luminescence of two generations. The cement of the first generation radiates very weak brownish red or no light, and that of the second generation send forth weak brownish red (Figure 14(f))

(4) Calcite that fills fractures is extremely weak in luminescence (Figures 14(d), 14(j), and 14(p)). There is no light from the inside of the horse-tooth shaped calcite cement on the wall of dissolution pore, but its edge has medium-strong orange red. The granular calcite that fills the middle part of the pore produces very weak-weak brownish red light, and their intensity is generally weaker than that of the surrounding micritic matrix

Table 1: EPMA of reef limestone.

Sample	Types of reef limestone and luminescence intensity	Na_2O	MgO	CaO	BaO	SrO	SiO_2	FeO	MnO	TiO_2	CO_2	FeO/MnO
Figure 12(b)	*Tubiphytes*, medium orange red	0.015	0.865	54.427	0.053	0.058	0	0.038	0.036	0	43.753	1.06
	Clasts wrapped by *Tubiphytes*, weak light	0.02	0.731	54.935	0	0.007	0	0.035	0.003	0	43.95	11.67
	Cement which fills pores, whose core is nonluminescent	0.017	0.607	53.742	0	0.048	0.821	0.086	0	0.016	44.144	—
	Cement which fills pores, whose edge gives off bright red	0.035	0.272	56.438	0	0.037	0	0	0.058	0.016	44.681	—
Figure 12(d)	Sea urchin spines, nonluminescent-very weal light	0.042	0.737	54.788	0.015	0.055	0	0.068	0.032	0	43.919	2.13
		0	0.881	53.58	0.063	0.056	0.661	0.166	0.027	0.024	44.165	6.15
	Sea urchin spines, medium luminescent	0.012	1.27	53.899	0.034	0	0	0.019	0.056	0	43.75	0.34
		0.007	1.244	53.718	0	0	0	0.005	0.02	0	43.536	0.25
Figure 12(e)	Micrite which fills the cavities of bryozoans, without being recrystallized	0.049	0.904	53.172	0.185	0.041	0	0.077	0.068	0.023	42.935	1.13
	Spar (recrystallized from micrite) which fill the cavities of bryozoans;	0.012	0.663	52.363	0.047	0.101	0	0.432	0.041	0.023	42.198	10.54
Figure 12(h)	Brachiopods, nonluminescent	0.159	0.358	54.885	0	0.186	0	0.038	0.025	0	43.693	1.52
	Subascosymplegma, whose bones are nonluminescent	0.224	0.464	55.247	0	0.174	0	0.011	0	0.024	44.128	—

5. Discussion

5.1. Correlation between Reef Development and Sea Level Change. The value of $\delta^{18}O$ and the correlation of C-O isotopes can roughly indicate the degree of diagenetic transformation of the sample. For instance, when $\delta^{18}O < -10‰$, it suggests that the sample has undergone strong diagenesis and can hardly represent the original C-O isotopic composition. Table 1 shows that the $\delta^{18}O$ value of most samples is >-10 ‰, and the correlation of C-O isotopes is <0.5 (Figure 11); in other words, their degree of diagenetic transformation is rather low and thus can be regarded as representatives of the original C-O isotopic composition.

On the other hand, the factors which affect the value of $\delta^{13}C$ of marine carbonate rocks are many, including sea level change, organic carbon content and burial rate, seawater temperature and salinity, and atmospheric water. Among them, the burial rate of organic carbon is the most important one. Because organic carbon is often rich in ^{12}C, more ^{12}C entered the organic carbon when a large amount of it was rapidly buried, and thus, the ^{13}C value of contemporaneous marine carbonate rocks switched to be positive, and vice versa. While the sea level was rising, the buried amount of organic carbon was increasing and the amount of organic carbon in the water was decreasing significantly. Since the CO_2 dissolved in seawater contained a large amount of ^{13}C, the resultant carbonate rock is also rich in ^{13}C, hence the high value of $\delta^{13}C$. On the contrary, while the sea level was declining, it corresponds to the low value of $\delta^{13}C$.

Apparently, it is in the context of the sea-level rising in the Late Carboniferous-Early Permian that the Keziliqiman reef in the Sangzhu section in the southwest Tarim Basin took shape. At that time, reef building organisms such as corals, *Colospongia*, and *Bryozoans* were flourishing. When they died, they were quickly buried, thus absorbing a large amount of ^{12}C, resulting in the relative enrichment of ^{13}C in seawater. However, the value of $\delta^{13}C$ of the straticulate dolostone in the exposed zone of the reef cap rapidly decreases to 0.119‰, which is consistent with the carbon isotopic characteristics of tidal flat dolostone. This suggests that when the reef cap was developing, the sea level dropped sharply, and the sedimentary environment in the Sangzhu area changed from the platform margin to a hot and dry supratidal zone. In this environment, reef building organisms such as corals, sponges, and *Bryozoans* could hardly survive, weakening the biological action in the sea and leading to the loss of ^{13}C in seawater and the eventual death of the reef. According to previous studies, the Early Permian (Cisuralian) was the continuation of the Carboniferous-Permian Glacial Period, when the climate was cold, suitable for cold water fauna to grow. As has been mentioned earlier, there were small nondissepimented corals adaptable to cold water in the Sangzhu front reef, and the values of $\delta^{13}C$ of the reef cap drop sharply—these two factors most likely point to this glacial period. The regression in the middle-late Early Permian in southwest Tarim Basin is also likely to be related to this period.

5.2. Reef's Evolution

5.2.1. Forming of the Reef Base. The warm and clear shallow water attracted huge numbers of echinoderms and *Fusulinina* to settle, and then sea urchins and crinoids reproduced abundantly until there formed an echinoderm shoal. However, without hard skeletons, those organisms were easily broken by waves when they died. Then, the spicules of their osseous lamella would disintegrate, and the spines of sea urchins would fall off, both constituting important sources of carbonate sediments. At this time when the water body was relatively deep, the hydrodynamic force was not quite strong; in other words, the environment was conducive for

echinoderms to accumulate in situ and form a positive geomorphic hump. This is a countermeasure against water depth, thus allowing bioclasts to be exposed to more light and oxygen. The echinoderm shoal constituted a desirable location for reef-building organisms to occur (Figure 15(a)).

5.2.2. Stage of Sponges as Reef-Building Organisms. The sea level was rising. On the echinoderm shoal that had developed earlier, reef-building organisms (e.g., *Colospongia*) began to multiply in the light-penetrating shallow zone until a "sponge jungle" (colony) came into being, or rather, sponges had taken over the entire shallow area. Meanwhile, sponges, *Tubiphytes*, and calcareous algae, in a combined effort, formed tangled grids to bond and bar all types of marl and bioclasts. The massive multiplication of *Colospongia* furnished the necessary hard ground for *Bryozoans* to grow on and adhere to; the grid structures of *Bryozoans* also barred and collected carbonate particles and marl. As a result, the geomorphic hump became increasingly prominent, and a sponge barrier reef gradually came into existence (Figure 15(b)).

5.2.3. Stage of Organic Diversification. The sea level continued to rise, and its hydrodynamic force grew gradually. In this context, colonial *Tetracoralla* that were adaptable to a turbulent water body began to settle, whereas *Colospongia* declined in number. Moreover, with the emergence of colonial *Tetracoralla* "jungle," marl and various bioclasts were easily barred and collected, resulting in the "growth" of the geomorphic hump (Figure 15(c)). Then, as the high-energy waves winnowed out the marl, bioclasts gathered in a relatively large amount around the colonial *Tetracoralla*. Moreover, since *Bryozoan* skeletons were brittle and tended to be broken by waves, their fragments constituted an important source of the sediments in the upper zone of the reef core. Meanwhile, small nondissepimented solitary corals (or *Cyathaxoniidae*), which were adaptable to a quite low-temperature environment, also occurred. In this way, the reef was growing taller, and the hydrodynamic forces of the water body on both sides of the reef began to assume different aspects, hence the distinction of front reef and back reef (Figure 15(d)).

5.2.4. Stage of the Reef's Death. With the sea level falling rapidly and the ambient temperature rising, the reef was exposed to hot and dry air in Sangzhu. This means that they had lost the basis for survival, resulting in the mass death of building organisms. In their place, algae began to flourish. In this context, parasyngenetic dolomitization and reflux seepage dolomitization tended to occur, thus the interbedding of algal limestone and dolomite emerged (Figure 15(e)).

5.3. Diagenesis of the Reefs

5.3.1. Controlling Diagenetic Factors. In general, the micritic matrix of Keziliqiman reef limestone in Sangzhu section has weak-medium CL, indicating that the marine fluid with low Mn content plays a leading role in its diagenetic process. The CL of some parts which were transformed by local recrystallization (neomorphism) is very weak-none; this may be related to atmospheric water, whose impact, though, was relatively limited. In addition, different types of bioclasts, different particles of the same type, and even different parts of the same bioclastic particle vary considerably in the intensity of luminescence, while the surrounding micritic matrix is basically the same in intensity. This observation indicates that the

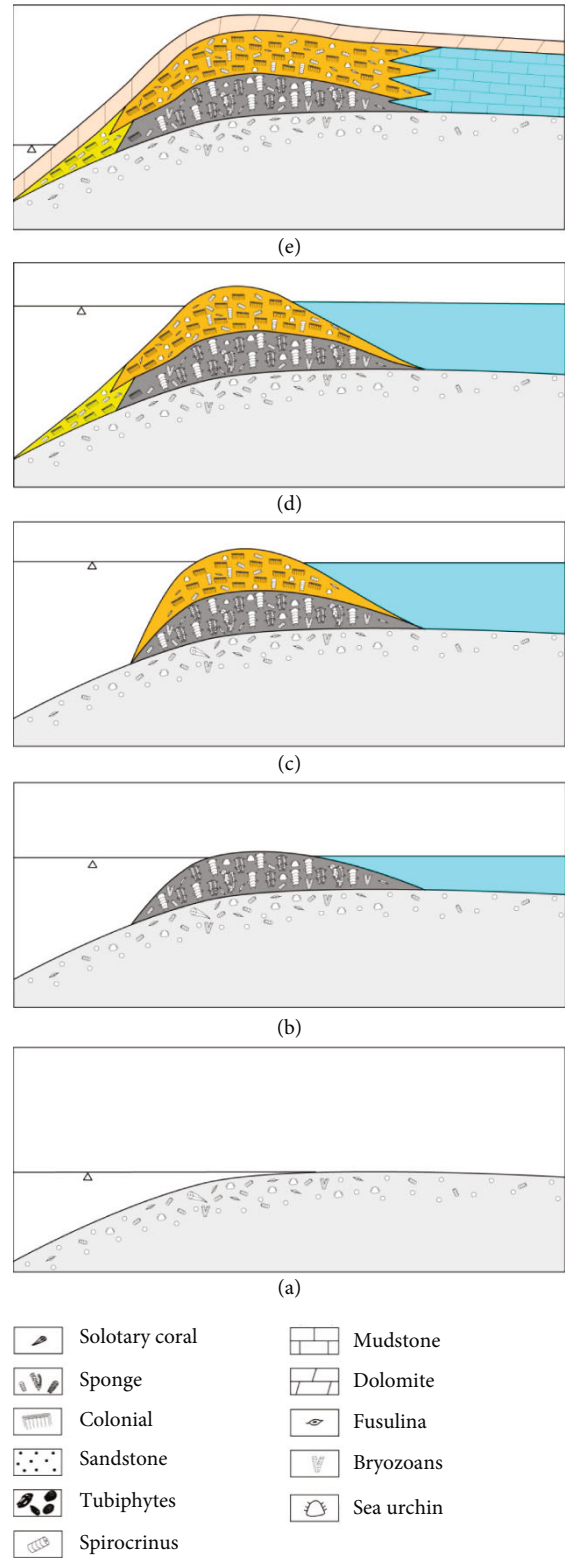

Figure 15: Evolution model of the Permian Keziliqiman Formation reef at Sangzhu section in Pishan.

nonmarine fluid with high Mn content features a certain degree of "fabric selectivity" in the transformation of the Sangzhu reef; the fabric selectivity mainly occurred in bioclastic particles rather than in the micritic matrix.

5.3.2. Diagenetic Stages

(1) Penecontemporaneous-contemporaneous diagenetic stage: recognizable diagenetic signs in the reef limestone of the Keziliqiman Formation of the Sangzhu section are as follows: (a) powdery-fine-crystalline dolostone, which is the best developed dolostone type in the reef, mainly of euhedral-semi-euhedral crystals. It formed from the skeletons of selectively displaced *Colospongia* (Figure 5(d)); (b) enveloping of algae and binding and wrapping of organisms by *Tubiphytes*; (c) burrow holes, which are typically filled by micrite, which is mainly aragonite or high magnesium calcite (most micrite is weakly luminescent, and some bioclasts give off very weak-no light, an indication of seawater with low Mn content); (d) the early extended edges of some echinoderms, which have very weak emission (Figure 14(e)); and (e) micritization of some sponge bones, which have none-weak brownish red emission

(2) Early diagenetic stage: the reef limestone of the Keziliqiman formation in Sangzhu mainly experienced phreatic fresh water and freshwater vadose environment. The main diagenetic signs of freshwater vadose environment include the following: (a) Sparry calcite cement fills intergranular and intragranular dissolution pores (Figures 14(b) and 14(n)). Their CL is often annular, or rather, their cores are nonluminescent or weakly luminescent while their edges are bright; this characteristic is typical of freshwater cements. (b) There are coaxially extended edges of echinoderms in multiple stages (Figure 14(e)). Echinoderms developed in the marine vadose environment. Their coaxially extended edges which continued to grow in freshwater vadose environment usually emit stronger luminescence than the first-stage cement due to the relatively high Mn content. (c) Fabric selective dissolution include some echinoderms which were entirely dissolved and then refilled, with only contours left. (d) In recrystallization, micrite was transformed into spar, and unstable components such as aragonite or magnesium calcite were changed into low magnesium calcite through neomorphism. For instance, the sparry cement which was transformed from the micrite which fills part of the ceolomic cavities is less luminescent than micrite. Some sea urchin spines were also recrystallized locally, and the luminescent intensity of the recrystallized part is higher than that of the original calcareous skeleton. The diagenetic signs of freshwater vadose environment mainly include nonfabric selective dissolution and geopetal structure (the micrite in the lower part emits weak-medium orange light, while the sparry calcite in the upper part is very weakly luminescent or non-luminescent)

(3) Middle-late diagenetic stage: its main diagenetic signs include the following: (a) concave-convex-suture contact between particles or organisms caused by chemical pressure dissolution and the local filling of calcite along the suture line; (b) lumpy and coarse-crystalline calcite growing in the center of dissolution pores, which is very weakly luminescent or non-luminescent (Figure 14(n)); and (c) the granular or lumpy calcite which fills structural fractures and which is very weakly luminescent or nonluminescent (Figures 14(d) and 14(p))

6. Conclusion

(1) In the Early Permian, when transgression in the southwest Tarim Basin reached the maximum range, a platform margin shoal of dozens of kilometers took shape. On the basis of the shoal developed the Keziliqiman Formation reef, a point reef growing along the platform margin. This reef can be divided into five sedimentary facies units: reef base, reef core, front reef, back reef, and reef cap. The lower zone of the reef core had colonial *Tetracoralla* as its dominant building organisms, and its lithology is typically coral framestone. The upper zone of the core had *Colospongia* as its dominant building organisms, and its lithology is typically sponge bafflestone. In this growth process, *Cyanobacteria* and *Tubiphytes* also played important roles in bonding

(2) Evolution of the Keziliqiman Formation reef in the Sangzhu section was mainly subjected to the sea-level rise or fall. When the sea level was rising, echinoderms and *Fusulinina* found the water depth, light and heat agreeable, and they began to inhabit the sandy shoal to form the reef base. On this base, *Colospongia* and corals have successively participated in reef building, thus the core took shape, and gradually, there emerged the front reef and the back reef. Subsequently, with the rapid decline of the sea level, the Sangzhu area became a hot and dry supratidal zone, where algae flourished and reef building organisms died en masse, until the reef died

(3) Stratigraphic lithology of Sangzhu section varies considerably; the reef is located in the top zone of Keziliqiman Formation, whereas 5.4 m upward is the continental purplish red mudstone at the bottom of Pusige Formation. It can be theorized that the sea level in southwest Tarim Basin declined quite fast. Then, considering the emergence of small nondissepimented corals adaptable to the cold water environment in the Sangzhu front reef, the regression in southwest Tarim Basin in the middle-late Early Permian is likely to be related to glaciers of this epoch. Therefore, the development of the Keziliqiman Formation reef can be regarded as the "last

glory" before the large-scale Early Permian regression occurred in southwest Tarim Basin

(4) Generally speaking, the Keziliqiman Formation reef is not significantly transformed by diagenesis. However, the diagenetic transformation in different zones of the reef and that of different types of sediment show apparent heterogeneity. The reef core manifests the biggest extent of transformation, involving dolomitization of *Colospongia* skeletons, the creation of secondary pores through dissolution, the change of some micritic matrix into spar through neomorphism, and the refilling of secondary pores by sparry cement. The back reef and front reef were less affected, but some bioclastic particles (such as of bryozoans, and echinoderms) have also assumed different degrees of neomorphic deformation. Moreover, in the diagenetic process, marine fluids played a leading role, because nonmarine fluids mainly exerted effect on bioclastic particles rather than on micritic matrix

Data Availability

The figures and tables used to support the findings of this study are included in the article.

Conflicts of Interest

The authors declare that they have no conflicts of interest.

Acknowledgments

The authors would like to show sincere thanks for those techniques which have contributed to this research.

References

[1] H. A. Stiff and L. E. Davis, "A method for predicting the tendency of oil field waters to deposit calcium carbonate," *Journal of Petroleum Technology*, vol. 4, no. 9, pp. 213–216, 1952.

[2] S. Chaudhuri, V. Broedel, and N. Clauer, "Strontium isotopic evolution of oil-field waters from carbonate reservoir rocks in Bindley field, Central Kansas, U.S.A," *Geochimica et Cosmochimica Acta*, vol. 51, no. 1, pp. 45–53, 1987.

[3] M. Bai, Z. Zhang, X. Cui, and K. Song, "Studies of injection parameters for chemical flooding in carbonate reservoirs," *Renewable and Sustainable Energy Reviews*, vol. 75, pp. 1464–1471, 2017.

[4] A. S. Alsharhan, "Geology and reservoir characteristics of carbonate buildup in giant Bu Hasa oil field, Abu Dhabi, United Arab Emirates," *AAPG Bulletin*, vol. 71, no. 10, pp. 1304–1318, 1987.

[5] M. F. Mady, A. Bagi, and M. A. Kelland, "Synthesis and evaluation of new bisphosphonates as inhibitors for oilfield carbonate and sulfate scale control," *Energy & Fuels*, vol. 30, no. 11, pp. 9329–9338, 2016.

[6] R. A. Dawe and Y. Zhang, "Kinetics of calcium carbonate scaling using observations from glass micromodels," *Journal of Petroleum Science and Engineering*, vol. 18, no. 3-4, pp. 179–187, 1997.

[7] R. L. Liu, N. Li, Q. F. Feng, C. Hai, and K. W. Wang, "Application of the triple porosity model in well–log effectiveness estimation of the carbonate reservoir in Tarim oilfield," *Journal of Petroleum Science and Engineering*, vol. 68, no. 1-2, pp. 40–46, 2009.

[8] E. Ukar, V. Baqués, S. E. Laubach, and R. Marrett, "The nature and origins of decametre-scale porosity in Ordovician carbonate rocks, Halahatang oilfield, Tarim Basin, China," *Journal of the Geological Society*, vol. 177, no. 5, pp. 1074–1091, 2020.

[9] H. Cheng, J. Wei, and Z. Cheng, "Study on sedimentary facies and reservoir characteristics of Paleogene sandstone in Yingmaili Block, Tarim Basin," *Geofluids*, vol. 2022, 14 pages, 2022.

[10] J. K. Smith, M. Yuan, T. H. Lopez, M. Means, and J. L. Przybylinski, "Real-time and in-situ detection of calcium carbonate scale in a West Texas oil field," *SPE Production & Facilities*, vol. 19, no. 2, pp. 94–99, 2004.

[11] Z. K. Hou, H. L. Cheng, S. W. Sun et al., "Crack propagation and hydraulic fracturing in different lithologies," *Applied Geophysics*, vol. 16, no. 2, pp. 243–251, 2019.

[12] H. Cheng, P. Ma, G. Dong, S. Zhang, J. Wei, and Q. Qin, "Characteristics of carboniferous volcanic reservoirs in Beisantai Oilfield, Junggar Basin," *Mathematical Problems in Engineering*, vol. 2022, 10 pages, 2022.

[13] J. Wei, H. Cheng, B. Fan, Z. Tan, L. Tao, and L. Ma, "Research and practice of "one opening-one closing" productivity testing technology for deep water high permeability gas wells in South China Sea," *Fresenius Environmental Bulletin*, vol. 29, no. 10, pp. 9438–9445, 2020.

[14] H. S. Al-Mimar, S. M. Awadh, A. A. Al-Yaseri, and Z. M. Yaseen, "Sedimentary units-layering system and depositional model of the carbonate Mishrif reservoir in Rumaila oilfield, Southern Iraq," *Modeling Earth Systems and Environment*, vol. 4, no. 4, pp. 1449–1465, 2018.

[15] X. Wei, Y. Guo, H. Cheng et al., "Estimation of fracture geometry parameters and characterization of rock mass structure for the Beishan Area, China," *Acta Geologica Sinica-English Edition*, vol. 94, no. 5, pp. 1381–1392, 2020.

[16] G. P. Eberli, G. T. Baechle, F. S. Anselmetti, and M. L. Incze, "Factors controlling elastic properties in carbonate sediments and rocks," *The Leading Edge*, vol. 22, no. 7, pp. 654–660, 2003.

[17] C. Lixin, Y. Haijun, C. Hanlie et al., "Logging identification of asphaltenes in carbonate reservoirs—taking the case of the Halahatang Oil Field as an example," in *International Field Exploration and Development Conference*, pp. 926–931, Singapore, 2020.

[18] X. Wei, Y. Guo, H. Cheng et al., "Rock mass characteristics in Beishan, a preselected area for China's high-level radioactive waste disposal," *Acta Geologica Sinica-English Edition*, vol. 93, no. 2, pp. 362–372, 2019.

[19] M. K. Gingras, B. MaCmillan, and B. J. Balcom, "Visualizing the internal physical characteristics of carbonate sediments with magnetic resonance imaging and petrography," *Bulletin of Canadian Petroleum Geology*, vol. 50, no. 3, pp. 363–369, 2002.

[20] P. G. Fookes and I. E. Higginbottom, "The classification and description of near-shore carbonate sediments for engineering purposes," *Geotechnique*, vol. 25, no. 2, pp. 406–411, 1975.

[21] F. G. Stehli and J. Hower, "Mineralogy and early diagenesis of carbonate sediments," *Journal of Sedimentary Research*, vol. 31, no. 3, pp. 358–371, 1961.

[22] F. T. Mackenzie and J. D. Pigott, "Tectonic controls of Phanerozoic sedimentary rock cycling," *Journal of the Geological Society*, vol. 138, no. 2, pp. 183–196, 1981.